Hindawi
Journal of Sensors
Volume 2024, Article ID 6690983, 9 pages
https://doi.org/10.1155/2024/6690983

Research Article

A Passive Wireless Smart Washer for Locking Force Monitoring on the Orthopedic Pedicle Screw

Che-Fu Liu,[1] **Tze-Hong Wong**,[2] **Hsin-Chuan Wang**,[1] **Asher Sun**,[1] **and Wensyang Hsu**[1]

[1]*Department of Mechanical Engineering, National Yang Ming Chiao Tung University, Hsinchu, Taiwan*
[2]*Department of Orthopedics, National Taiwan University Hospital Hsinchu Branch, Hsinchu, Taiwan*

Correspondence should be addressed to Wensyang Hsu; whsu@nycu.edu.tw

Received 29 August 2023; Revised 15 March 2024; Accepted 13 April 2024; Published 17 May 2024

Academic Editor: Rajkishor Kumar

A pedicle screw is a component for fixation in spine fusion surgery, often for patients with osteoporosis. Spine fusion condition highly depends on whether the pedicle screw is tightly fixed on spine, if not, spine fusion will not work properly. After the surgery, the first 3 months is the most crucial period, and bone healing situation cannot be shown through X-ray before the first radiologic images taken around the sixth week. Therefore, it is helpful to have a nonradiative method to monitor the locking force of the pedicle screw after surgery, especially during the early stage. Here a passive wireless force sensor is developed for monitoring the locking force of the pedicle screw, as we call it a smart washer. By integrating a capacitive ring-shape force sensor with an inductor, a passive LC sensor can be built by measuring the resonant frequency wirelessly. The smart washer is designed and calibrated to establish the relation between the locking force and resonant frequency, and then it is fixed with a screw in a porcine femur, with and without medium between the reader and inductor. When the locking force decreases from 8.3 to 0.9 N, the error is less than 0.5 N, and the maximum wireless sensing distance is 72 mm. However, the medium between the reader and the sensor inductor will affect the resonant frequency, but not the sensitivity. Therefore, the locking force variation can still be calculated by the resonant frequency shift accurately. Furthermore, by designing another five LC sensors with different operating resonant frequency ranges, it is possible to identify locking forces at different locations for more pedicle screws. To our knowledge, no LC force sensor was proposed to monitor the locking force of pedicle screws after surgery in the past.

1. Introduction

In orthopedics, due to people's aging, there are a lot of diseases and accidents to cause bones fracture, degenerative, infection, and inflame. To help patients with these diseases and accidents, diagnosis, treatment, and postsurgical monitoring are all very important. In orthopedic treatments, the orthopedic screws are often used for bones fixation and realign. Unfortunately, there is some probability of the orthopedics screws to become loose, which may make orthopedic treatment failure and bone-screw-related complications, including infection and inflammation [1–4]. To reduce risk of orthopedic screws loosen, improving orthopedic screws fixation [5–8] and monitoring orthopedic screws loosen status [9, 10] are desired.

For instance, the pedicle screw system is one of the most common methods in spinal fusion surgery. The purpose is to fix the patient's vertebra in place to maintain its stability for the bones to heal. The first 3 months after the surgery is the most crucial period during the healing process. Thus, the condition of the pedicle screw fixation in the bone affects the outcome directly. In current clinical practice, X-ray-based images are used to check bone healing and the condition of the screw, including static radiographs [11], dynamic radiographs [12], and computed tomography [13]. Since spinal fusion [14] takes time, X-ray images are usually taken 6 weeks after the surgery, and it is not recommended to have X-ray examinations frequently in a short period of time. However, there is a fair chance of pedicle screw loosening after surgery that causes unsatisfactory recovery. Therefore, a nonradioactive method will be helpful to check the fixation statuses earlier and more regularly during the first 3 months.

To implant a sensor in human body to measure locking force of pedicle screw, remotely wireless sensing is preferred. Without a battery attached to the sensor, a passive sensor,

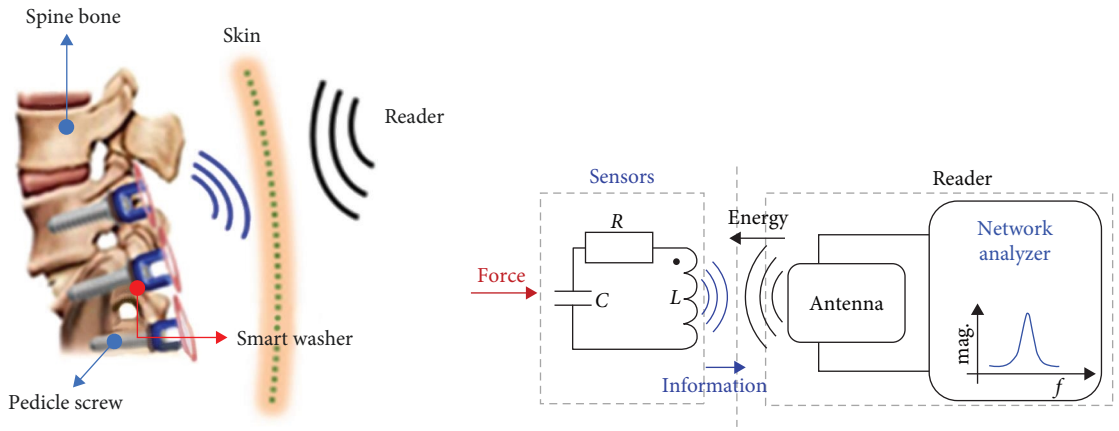

Figure 1: Operating principle: (a) schematic illustrations of wireless sensing for monitoring locking force of the pedicle screw and (b) principle of wireless LC sensor.

it is smaller and safer. Therefore, a wireless passive sensing device is suitable to be implanted in human body for measuring locking force of a pedicle screw. Various sensing principles were proposed to measure the locking force of a screw, such as piezoelectric [15], piezoresistive [16, 17], and piezomagnetic [18]. However, those devices are active and wired devices, not suitable to be placed inside the human body. A passive wireless vibroacoustic device [19] was proposed to measure relative distance between orthopedic pedicle screws and bones to decide the loosening status of pedicle screws during surgery. However, it is not suitable after surgery to monitor the loosening status of pedicle screws.

LC (inductor and capacitance) sensors could be passive and wireless, and many design improvement schemes were proposed [20–30]. Some of them were proposed for wireless sensing in harsh environment, including sensing pH in chemical environment [20], working at high-temperature environment [21–23]. Some of them were proposed for sensing physical properties, including monitoring structural health [24], sensing multiple physical quantities by one sensor [25–28]. Furthermore, some of them were proposed for sensing bioinformation, including measuring blood pressure in discussing the feasibility bioapplication [29] and eye pressure with biocompatibility [30]. However, to our knowledge, no LC force sensor was proposed to monitor the locking force of pedicle screws after surgery.

Here, a passive wireless LC sensor, as we call it a smart washer, is developed to show the feasibility to detect the locking force of the pedicle screw. The proposed smart washer does not require a battery and can measure the locking force remotely, as shown in Figure 1(a). It is based on the LC technology. When the locking force variation induces the capacitive change on the force sensor, the resonant frequency of the LC circuit changes as well, as listed in Equation (1). By measuring the resonant frequency shift by an external reader, the variation on locking force can be identified as well, as shown in Figure 1(b). The proposed a nonradioactive approach has great potential to help medical staffs to inspect the condition of the pedicle screw fixation in bones after surgery:

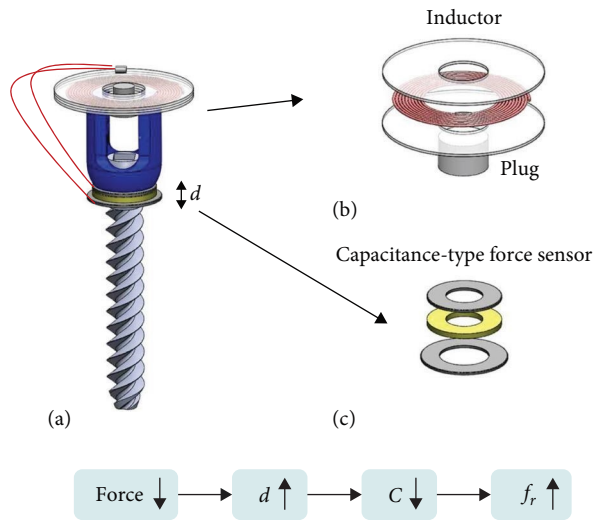

Figure 2: Concept design: (a) schematic illustration of the wireless sensor on the pedicle screw, including (b) the inductor and (c) capacitive force sensing ring.

$$f = \frac{1}{2\pi\sqrt{LC}}, \tag{1}$$

where f is the resonant frequency, L is the inductor, and C is the capacitance.

2. Materials and Methods

2.1. Concept Design. The proposed LC sensor includes a flat inductor and a capacitive force sensing ring like a washer, as shown in Figure 2. When the distance between two plates in a parallel-plate capacitor changes, the capacitance also varies according to Equation (2), as well as the resonant frequency:

$$C = \frac{A\varepsilon}{d}, \tag{2}$$

where A is the overlap area of two plates, d is the distance of two plates, and ε is the dielectric constant of the material between two plates.

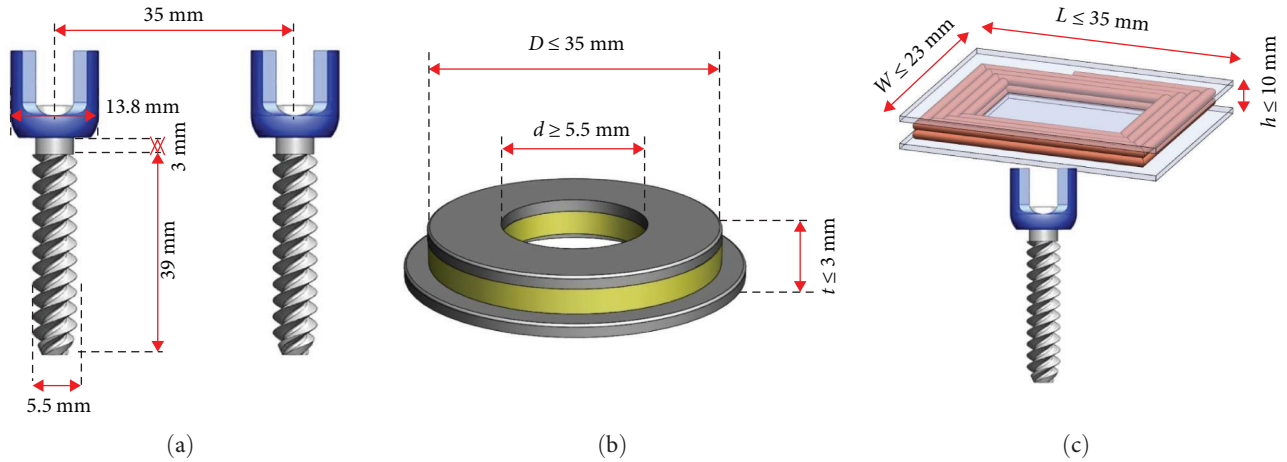

FIGURE 3: Dimensions and constraints: (a) dimensions of the pedicle screw; (b) constraints on the capacitive force sensor; and (c) constraints on the inductor.

As Figure 2 illustrates, the flat inductor with a plug is mounted on the top of the pedicle screw to reduce the distance to the skin surface, and the capacitive force ring is placed under the rod holder. The inductor and the capacitive sensor are connected through wires to form the LC loop. After the pedicle screw is fixed on the bone with the desired locking force, a corresponding resonant frequency can be measured. If the screw loosens, the distance between the two plates in the capacitive sensor will increase. Then the capacitance becomes smaller, which leads to the increase of the resonant frequency.

As shown in Figure 3(a), the pedicle screw used here has a diameter of 5.5 mm, including the whorls. The length of the screw is 39 mm, with 3 mm containing no whorls. During surgery, screws are used in pairs, and certain distances are required between two pedicles in both directions. Figures 3(b) and 3(c) illustrate the dimensional constraints on the capacitive sensor and the inductor. For a longer wireless sensing distance, a larger antenna is preferred. The inductor is made of copper wire with diameter of 0.5 mm. There are six loops for the inductor, where the height $h = 1$ mm, length $L = 35$ mm, and width $W = 23$ mm. In addition, the inductor is wrapped in PDMS to ensure the biocompatibility. The initial inductance is calculated to be 2.68 μH by Equation (3) [31], and its measured value is 3.17 μH:

$$I = \frac{0.0276((W+L)N)^2}{1.908(W+L) + 9h + 10D_c}, \quad (3)$$

where N is number of loops, h is height of the inductor, and D_c is cooper wire diameter.

The capacitive force sensor consists of two metal plates and the dielectric layer between them. Two commercially available stainless washers are used as the plates. The upper plate has a 12.7 mm outer diameter, a 5.5 mm inner diameter, and 1 mm thickness. To prevent the lower plate from touching the pedicle screw (which would cause short-circuit of the capacitor), we use a lager washer of 6 mm inner diameter, 16 mm outer diameter, and the same 1 mm thickness. The biocompatible PDMS is the chosen dielectric material of the capacitive force sensor. The outer diameter is 16 mm which fits with the bottom plate and the inner diameter is 5.5 mm. The thickness of the dielectric layer is 1 mm, and the capacitance measured value is 3.6 pF, and the system capacitance is 5.41 pF.

2.2. Fabrication. Figure 4 depicts the fabrication process of the LC sensor. The copper wire is wrapped around the acrylic mold to form the inductor. To build a capacitive force sensor, the upper stainless plate is placed in the acrylic mold with PDMS poured in and then the bottom plate is placed on top. After the PDMS is solidified, the capacitive force sensor can be removed from the acrylic mold. By connecting the inductor and the capacitive sensor with the copper wire, the passive wireless LC sensor is built, as shown in Figure 5.

3. Testing Results

There are three types of tests. First, the calibration on sensor is performed to establish the relation between the locking force and the resonant frequency. In the second test, the LC sensor is fixed on a porcine femoral bone to investigate the sensor performance with and without extra tissue between the reader and the sensor. Finally, vibration tests are conducted to examine the variation of the locking force while loosening the pedicle screw gradually with a shaker.

3.1. Calibration. Figure 6 shows the experiment setup. A resistive force sensor (FSR-400) is adopted as a reference force sensor to measure the locking force of a screw fixed on a wood block. A network analyzer (Agilent 4395A) is used to read the resonant frequency. In the tests, the screw is screwed into the plate by hand as tight as possible and then is gradually turned loose. By performing this process three times, the results shown in Figure 7 are obtained. When the locking force decreases from 9.3 to 0 N, the resonant frequency shifts from 37.8 to 38.57 MHz. The sensitivity based on the fitted linear curve is 0.073 MHz/N. The wireless sensing distance between the reader and the sensor inductor

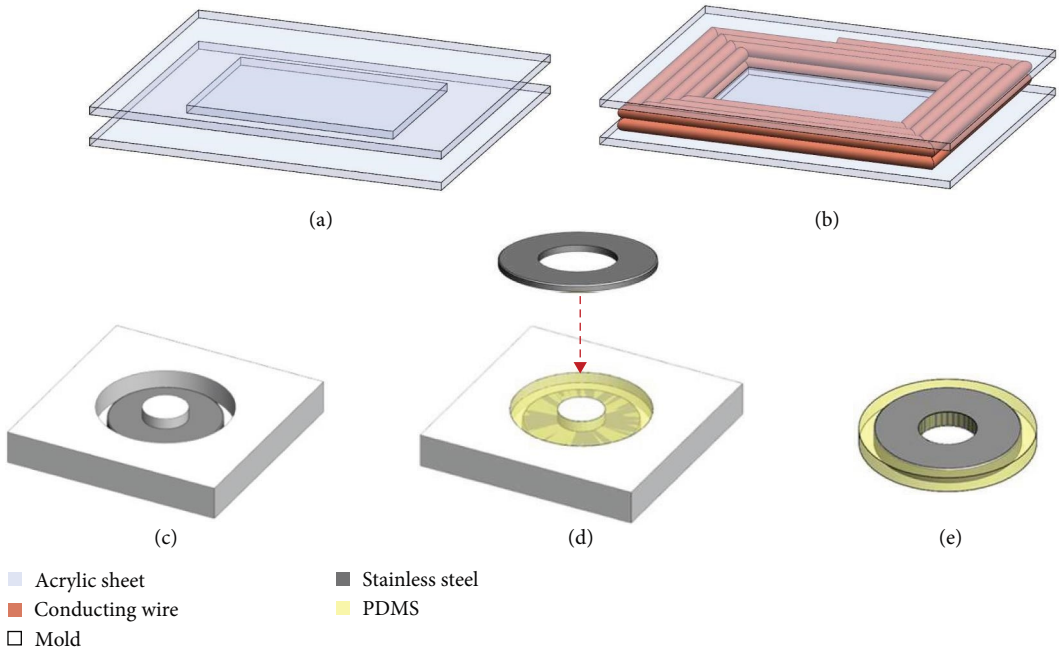

Figure 4: (a–e) Fabrication process of the inductor and the capacitive force sensor.

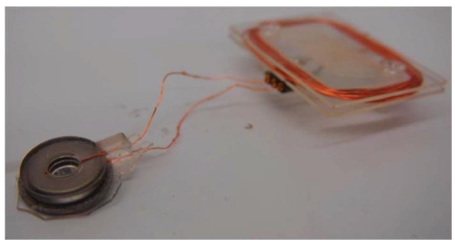

Figure 5: Fabricated prototype of the passive wireless locking-force sensor.

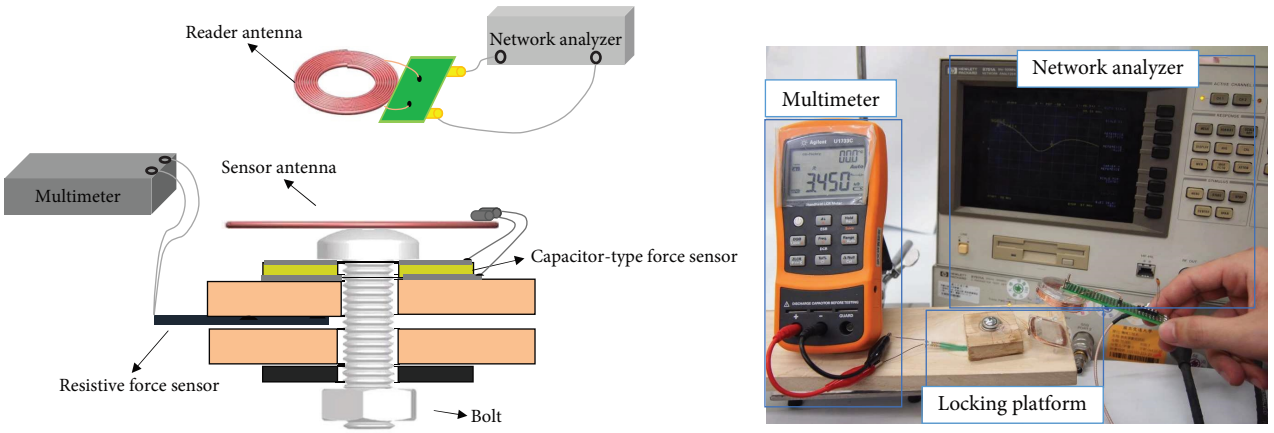

Figure 6: Calibration tests: (a) schematic illustration of the experiment setup on the locking platform to calibrate the relation between the locking force and the corresponding resonant frequency; (b) photograph of the experimental setup.

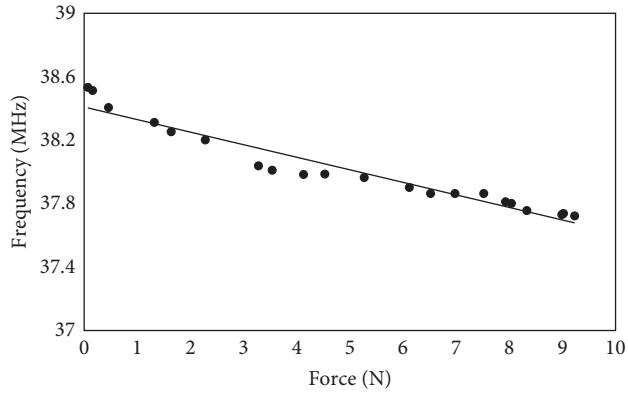

Figure 7: The measured resonant frequency with respect to different locking forces on the locking platform.

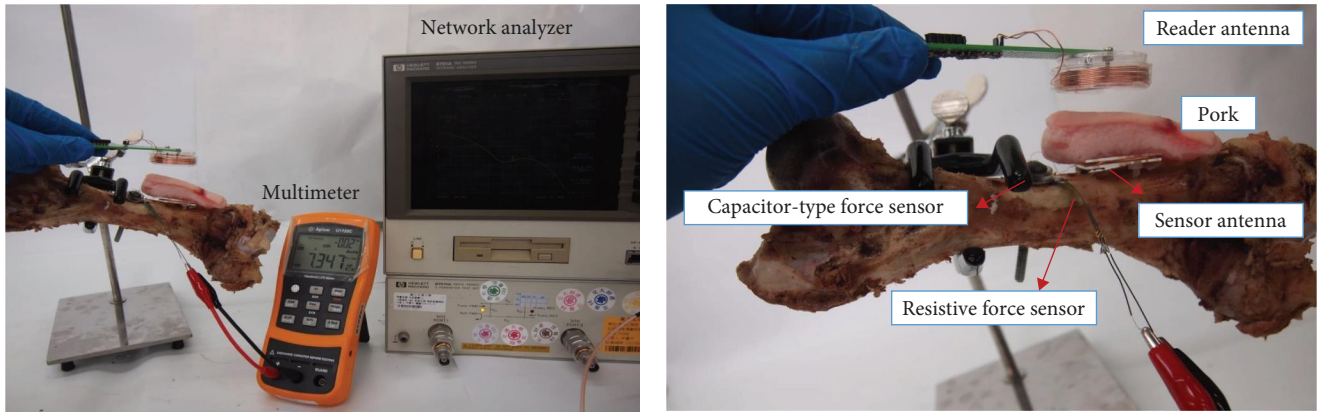

(a) (b)

Figure 8: Photographs of (a) the experiment setup used to measure the resonant frequency with different locking forces on femur with pork medium and (b) close-up of the sensing and reading devices.

can be up to 72 mm. The limit of detection of the sensor on locking force is 0.47 N where there is an evident frequency drop from the initial resonant frequency.

3.2. Locking Force Test on a Porcine Femur. After calibration, the device is tested on a porcine femoral bone to mimic the practical situation, as shown in Figure 8. A screw with the capacitive force sensor is fixed in the femur and a slice of 1.2-cm-thick pork is attached on top of the inductor. The relations between the locking force and the resonant frequency with and without the pork slice are shown in Figure 9. Without the pork slice, 9.0 N locking force induces 0.76 MHz frequency shift. The resonant frequency at 0 N locking force is 38.59 MHz, similar to the result of the calibration test. The sensitivity based on the fitted linear curve is 0.071 MHz/N, close to the sensitivity of 0.073 MHz/N in the calibration test.

3.3. Vibration Test. When the pedicle screw is installed, its locking force may vary due to the changes in bone mass (density) or the patient's daily movements. In this test, we apply external vibration to loosen the locking force of the bone screw, as shown in Figure 10. After integrating the pedicle screw and the sensing device, we lock the screw in the femur and fix the femur and the sensing device onto a vibration platform. Then, a continuous vibration with a frequency of 20 Hz and an acceleration of 4 m/s^2 is applied to the platform. The relations between the locking force and the resonance frequency are measured once every 30 min. The results are shown in Figure 11. When the vibration reaches 36,000 times, the locking force reduces from 8.3 to 8 N. The estimated value is very similar to the reference measured by the piezoresistive sensor. When the vibration comes to 72,000 times, the locking force reduces to 6 N, and the estimated value is 6.5 N. When it reaches 108,000 times, the locking force greatly reduces to 1.3 N, and the estimated value is 1.2 N. When the vibration is 144,000 times, the locking force reduces to 0.9 N.

4. Discussions

In the calibration test, while calculating the locking force from the resonant frequency, the absolute value of the locking force could be affected by the medium between the reader and the inductor, but the sensitivity is nearly the same. Therefore, the variation of the locking force still can be calculated by the resonant frequency shift.

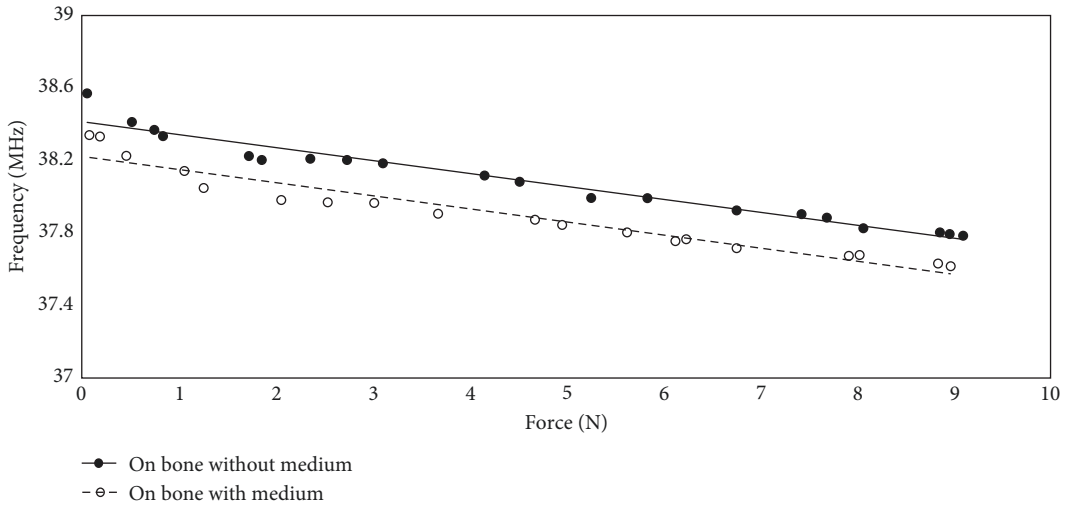

Figure 9: The experimental results of the resonant frequency correspond to the locking force on femur with and without the pork slice.

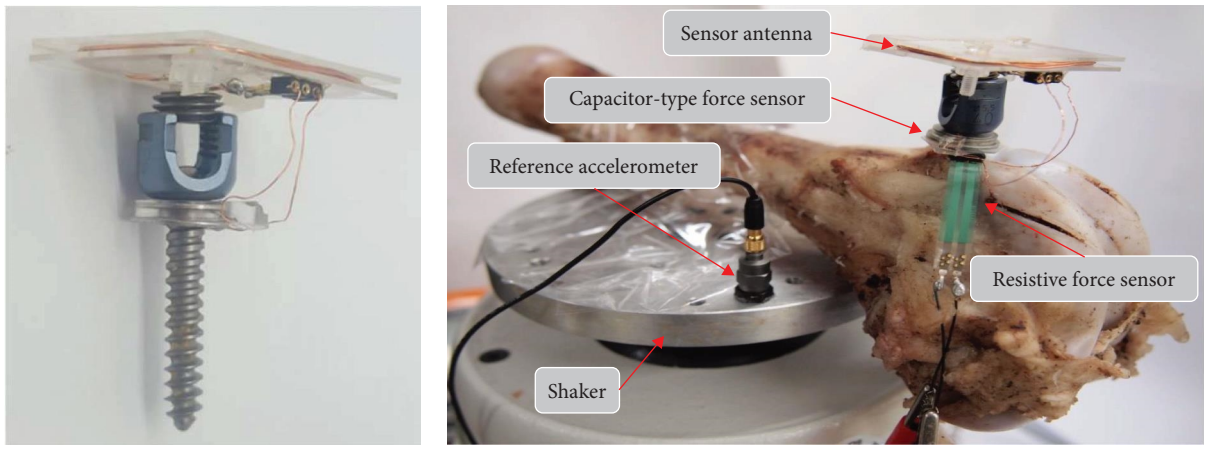

(a) (b)

Figure 10: Photograph of (a) the passive wireless sensing device mounted on the pedicle screw and (b) the experiment setup on the porcine femur in the vibration test.

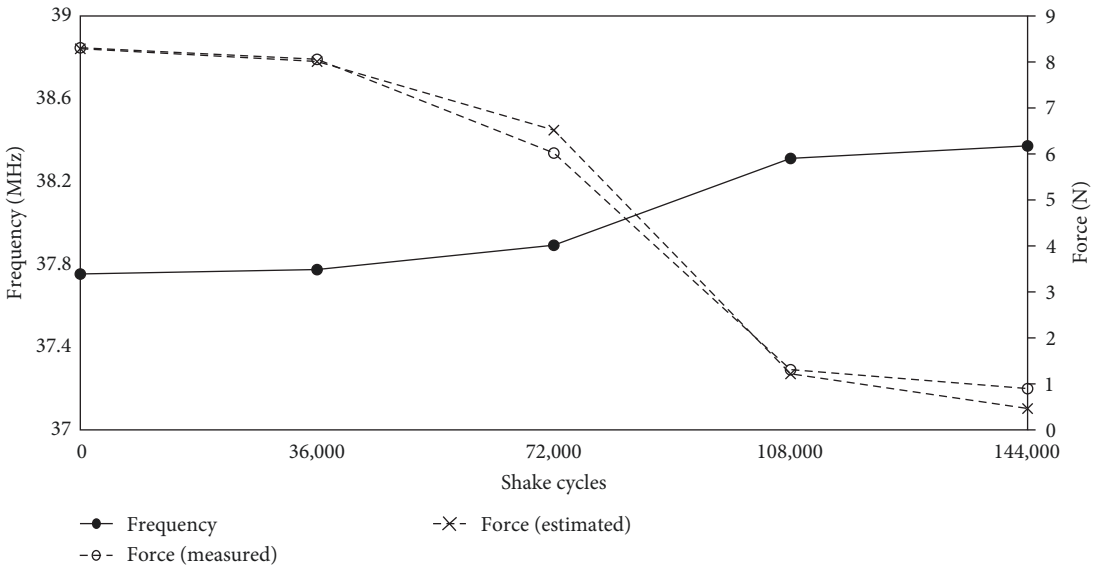

Figure 11: The experimental results of the vibration test.

Table 1: Six LC sensors with different resonant frequencies.

LC sensor type	$f1$	$f2$	$f3$	$f4$	$f5$	$f6$
Loops of inductor (turns)	6	9	12	15	18	21
Vertical height (mm)	1	1.5	2	2.5	3	3.5
Estimated inductance (μH)	2.68	4.12	7.66	12.45	18.00	27.82
Measured inductance (μH)	3.17	4.63	8.67	10.15	18.90	27.16
Measured frequency range (MHz)	38.43–37.61	33.34–32.61	22.47–21.89	20.71–20.26	12.28–11.91	10.11–9.79
Sensitivity (MHz/N)	0.078	0.069	0.057	0.042	0.034	0.029
Measured maximum wireless sensing distance (mm)	72	64	66	60	58	56

In the locking force test, when a slice of pork is placed between the reader and the LC sensors, the resonant frequency at 0 N becomes lower. However, the sensitivity is 0.072 MHz/N, very close to the sensitivity without the pork slice.

In the vibration test, the final measurement is compared to the initial measurement of 8.3 N, the change value is 7.4 N. The change of locking force estimated by the resonance frequency is 7.9 N. Compared to the measured change value (7.4 N), the error is 0.5 N. Within this resonance frequency range 37.75–38.37 MHz, the errors of the locking force between the estimated values and the direct measurements are all less than 0.5 N. It indicates that the variation of the locking force can be estimated with good accuracy by using the measured resonance frequency.

In general, the distance from the human spine to skin surface is about 30–60 mm [32, 33], and the maximum measurement distance 72 mm of our device is suitable for most cases, but may not suitable for seriously obese patients whose distance from spine to skin surface could reach 80 mm [33]. Furthermore, it is often to use more than one pedicle screw in surgery. The possibility of using multiple screws with LC sensors is discussed below.

4.1. Multiple LC Sensors Design. In spine surgery, it may need 4–6 pedicle screws. In order to identify the signals from different sensors, six LC sensors with different resonant frequencies are designed, as listed in Table 1, where all six LC sensors have the same capacitive force sensors, but different inductances.

When the locking force on the $f1$ sensor increases from 0 to 9.2 N, the resonant frequency of $f1$ LC sensor is decreased from 38.43 to 37.61 MHz. In order to make resonant frequency range of $f2$ sensor does not overlap with $f1$, the loops and height of $f2$ inductor are increased to 9 turns and 1.5 mm, respectively. Its estimated and measured values of inductance is 4.12 and 4.63 μH, respectively. Therefore, in locking force test, the resonant frequency range of $f2$ sensor is from 33.34 to 32.61 MHz, which does not overlap with $f1$. On the other hand, its sensitivity is 0.069 MHz/N, and its maximum wireless sensing distance is 64 mm.

By the similar procedure, the other four LC sensors with different resonant frequency ranges are designed, fabricated, and tested, as listed in Table 1. Among these six LC sensors, the maximum sensitivity is 0.078 MHz/N, and the minimum sensitivity is 0.029 MHz/N, and the farthest wireless sensing distance is 72 mm, and the shortest one is 56 mm.

4.2. Interference of Two Passive Wireless LC Sensors. When two passive wireless LC sensors are too close, it is possible to cause interference which makes resonant frequencies of LC sensors shift in sensing. To find the minimum separation distance of two sensors without interference, the inductor distance experiment of two sensors is carried out, as shown in Figure 12. Among the six passive wireless LC sensors, resonant frequencies of $f1$ and $f2$ are the closest, and resonant frequencies of $f1$ and $f6$ are the farthest. The interference experiment result with $f1$ sensor and $f2$ sensor is shown in Figure 12(b). It shows that when the separation distance S is 0.8 cm, the resonant frequency shift of $f1$ and $f2$ is about 0.2 MHz. When the separation distance is increased to 2 cm, the resonant frequency shift is almost 0 MHz. On the other hand, the minimum separation distance S is 1.2 cm for $f1$ and $f6$ two sensors, as shown in Figure 12(c). According to these results, at least 2 cm separation distance between these six LC sensors is enough to avoid interference in reading resonant frequency.

5. Conclusions

The pedicle screw system is for spinal fusion surgery. The first 3 months after the surgery is the most crucial period. Currently, the examination of the bone healing condition relies on the radiologic approach. A nonradiative method for monitoring the locking force of the pedicle screw on the bone after the surgery is favorable to check the fixation condition earlier and more frequently. This study proposes to use a passive wireless LC sensor for monitoring the pedicle screw's locking force by integrating a ring-shape capacitive force sensor and an inductor, as we call it a smart washer. When the locking force decreases, the capacitance of force sensor also decreases and the resonant frequency becomes higher. By measuring resonant frequency shift, the variation of the locking force can be estimated through the calibration curve. Our experiment results show that when the locking force decreases from 8.3 to 0.9 N, the error is less than 0.5 N. The maximum wireless sensing distance is 72 mm. However, the medium, referring to the pork slice in the test, between the reader and the inductor will affect the resonant frequency, but will not influence the sensitivity. Therefore, the absolute value

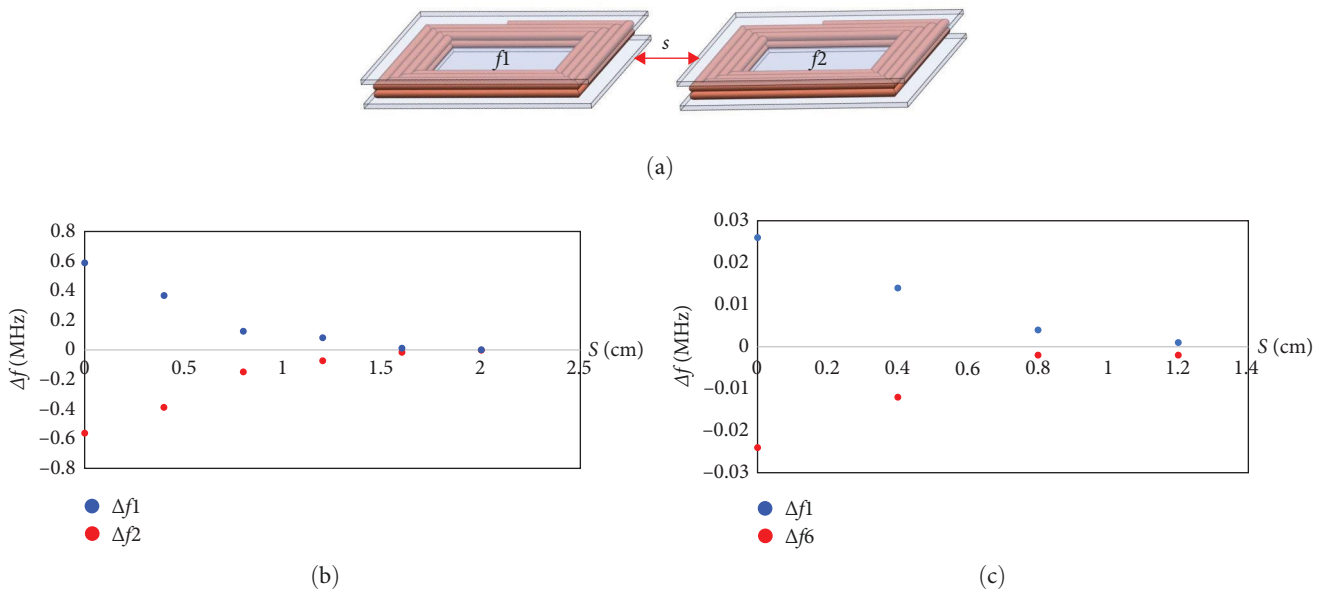

FIGURE 12: Interference measurement: (a) separation distance S of two inductors for $f1$ LC sensor and $f2$ LC sensor; (b) result with $f1$ and $f2$; and (c) result with $f1$ and $f6$.

of the locking force could be inaccurate due to the medium between the sensor and reader, but the locking force variation still can be calculated accurately by the resonant frequency shift. Another five LC sensors are also designed, fabricated, and tested to have different operating resonant frequency ranges. It is possible to identify locking forces at different locations with more pedicle screws.

Data Availability

Dataset will be made available upon request.

Conflicts of Interest

The authors declare that they have no conflicts of interest.

Acknowledgments

This study was supported by the Ministry of Science and Technology of Taiwan under grant number MOST 108-2221-E-009-082-MY2.

References

[1] R. Agarwal, V. Gupta, and J. Singh, "Additive manufacturing-based design approaches and challenges for orthopaedic bone screws: a state-of-the-art review," *Journal of the Brazilian Society of Mechanical Sciences and Engineering*, vol. 44, no. 1, Article ID 37, 2022.

[2] J. Wang, J. Chu, J. Song, and Z. Li, "The application of impantable sensors in the musculoskeletal system: a review," *Frontiers in Bioengineering and Biotechnology*, vol. 12, Article ID 1270237, 2024.

[3] M. D. Wild, S. Zimmermann, K. Klein et al., "Immediate stabilization of pedicle screws: preclinical pilot study of polymer-augmented pedicle screws," *Current Directions in Biomedical Engineering*, vol. 9, no. 1, pp. 13–16, 2023.

[4] M. R. Fasser, G. Gerber, C. Passaplan et al., "Computational model predicts risk of spinal screw loosening in patients," *European Spine Journal*, vol. 31, no. 10, pp. 2639–2649, 2022.

[5] L. Song, J. Xiao, R. Zhou, C.-C. Li, T.-T. Zheng, and F. Dai, "Clinical evaluation of the efficacy of a new bone cement-injectable cannulated pedicle screw in the treatment of spondylolysis-type lumbar spondylolisthesis with osteoporosis: a retrospective study," *BMC Musculoskeletal Disorders*, vol. 23, no. 1, Article ID 951, 2022.

[6] L.-C. Wu, Y.-Y. Hsieh, F.-Y. Tsuang, Y.-J. Kuo, and C.-J. Chiang, "Cutting flute and thread design on self-tapping pedicle screws influence the insertion torque and pullout strength," *Applied Sciences*, vol. 12, no. 4, Article ID 1956, 2022.

[7] M.-K. Hsieh, Y.-D. Li, Y.-C. Li et al., "Improved fixation stability for repairing pedicle screw loosening using a modified cement filling technique in porcine vertebrae," *Scientific Reports*, vol. 12, no. 1, Article ID 2739, 2022.

[8] D. Sanjay, J. S. Bhardwaj, N. Kumar, and S. Chanda, "Expandable pedicle screw may have better fixation than normal pedicle screw: preclinical investigation on instrumented L4-L5 vertebrae based on various physiological movements," *Medical & Biological Engineering & Computing*, vol. 60, no. 9, pp. 2501–2519, 2022.

[9] K. P. Iyengar, A. D. Kariya, R. Botchu, V. K. Jain, and R. Vaishya, "Significant capabilities of SMART sensor technology and their applications for industry 4.0 in trauma and orthopaedics," *Sensors International*, vol. 3, Article ID 100163, 2022.

[10] J. M. Spirig, R. Sutter, T. Götschi, N. A. Farshad-Amacker, and M. Farshad, "Value of standard radiographs, computed tomography, and magnetic resonance imaging of the lumbar spine in detection of intraoperatively confirmed pedicle screw loosening—a prospective clinical trial," *The Spine Journal*, vol. 19, no. 3, pp. 461–468, 2019.

[11] W. H. McAlister and G. D. Shackelford, "Measurement of spinal curvatures," *Radiologic Clinics of North America*, vol. 13, no. 1, pp. 113–121, 1975.
[12] A. A. Patel and W. R. Spiker, "Update on the diagnosis and treatment of lumbar nonunions," *Seminars in Spine Surgery*, vol. 20, no. 1, pp. 20–26, 2008.
[13] C. Goldstein and B. Drew, "When is a spine fused?" *Injury*, vol. 42, no. 3, pp. 306–313, 2011.
[14] L. K. Cannada, S. C. Scherping, J. U. Yoo, P. K. Jones, and S. E. Emery, "Pseudoarthrosis of the cervical spine: a comparison of radiographic diagnostic measures," *Spine*, vol. 28, no. 1, pp. 46–51, 2003.
[15] S. H. Conrad and W. P. Kistler, "Device for measuring the forces between components of an assembly," U.S. Patent No. 3151258, 1960.
[16] H. U. Baumgartner, R. Calderara, H. C. Sonderegger, and P. Weber, "Piezoresistive force-measuring element and it's use for determine forces acting on a component," U.S. Patent No. 4738146, 1986.
[17] H. C. Kropp, "Load washer," U.S. Patent No. 5222399, 1991.
[18] H. Kwun, "Load sensor for measuring engine cylinder pressure and seat occupant weight," U.S. Patent No. 6134947, 1997.
[19] M. Seibold, B. Sigrist, T. Götschi et al., "A new sensing paradigm for the vibroacoustic detection of pedicle screw loosening," arXiv preprint arXiv, 2210.16170, 2022.
[20] J. A. García-Cantón, A. Merlos, and A. Baldi, "A wireless LC chemical sensor based on a high quality factor EIS capacitor," *Sensors and Actuators B: Chemical*, vol. 126, no. 2, pp. 648–654, 2007.
[21] P. Jia, J. Liu, J. Qian, Q. Ren, G. An, and J. Xiong, "An LC wireless passive pressure sensor based on single-crystal MgO MEMS processing technique for high temperature applications," *Sensors*, vol. 21, no. 19, Article ID 6602, 2021.
[22] K. S. Varadharajan Idhaiam, J. A. Caswell, P. D. Pozo et al., "All-ceramic passive wireless temperature sensor realized by tin-doped indium oxide (ITO) electrodes for harsh environment applications," *Sensors*, vol. 22, no. 6, Article ID 2165, 2022.
[23] D. Marioli, E. Sardini, and M. Serpelloni, "Passive hybrid MEMS for high-temperature telemetric measurements," *IEEE Transactions on Instrumentation and Measurement*, vol. 59, no. 5, pp. 1353–1361, 2010.
[24] Y. Jia, K. Sun, F. J. Agosto, and M. T. Quiñones, "Design and characterization of a passive wireless strain sensor," *Measurement Science and Technology*, vol. 17, no. 11, pp. 2869–2876, 2006.
[25] M. Mustafa, M. Rizwan, M. Kashif, T. Khan, M. Waseem, and A. Annuk, "LC passive wireless sensor system based on two switches for detection of triple parameters," *Sensors*, vol. 22, no. 8, Article ID 3024, 2022.
[26] K. G. Ong, C. A. Grimes, C. L. Robbins, and R. S. Singh, "Design and application of a wireless, passive, resonant-circuit environmental monitoring sensor," *Sensors and Actuators A: Physical*, vol. 93, no. 1, pp. 33–43, 2001.
[27] K. G. Ong and C. A. Grimes, "A resonant printed-circuit sensor for remote query monitoring of environmental parameters," *Smart Materials and Structures*, vol. 9, no. 4, pp. 421–428, 2000.
[28] A. D. DeHennis and K. D. Wise, "A wireless microsystem for the remote sensing of pressure, temperature, and relative humidity," *Journal of Microelectromechanical Systems*, vol. 14, no. 1, pp. 12–22, 2005.
[29] K.-H. Shin, C.-R. Moon, T.-H. Lee, C.-H. Lim, and Y.-J. Kim, "Flexible wireless pressure sensor module," *Sensors and Actuators A: Physical*, vol. 123-124, pp. 30–35, 2005.
[30] P.-J. Chen, D. C. Rodger, S. Saati, M. S. Humayun, and Y.-C. Tai, "Microfabricated implantable parylene-based wireless passive intraocular pressure sensors," *Journal of Microelectromechanical Systems*, vol. 17, no. 6, pp. 1342–1351, 2008.
[31] F. E. Terman, *Radio Engineers' Handbook*, McGraw-Hill Book Company, Inc., 1943.
[32] G. R. Harrison and N. W. B. Clowes, "The depth of the lumbar epidural space from the skin," *Anaesthesia*, vol. 40, no. 7, pp. 685–687, 1985.
[33] M. M. Tactuk, R. S. Dux, Y. M. Díez, F. R. Simón, R. M. Martín, and M. G. Fernández, "ESRA19-0408 distance from skin to epidural space: correlation with anthropometric measurements," *Regional Anesthesia and Pain Medicine*, vol. 44, no. Suppl 1, pp. A192–A192, 2019.